Journal of Alloys and Compounds 509 (2011) 4341–4347

Contents lists available at ScienceDirect

Journal of Alloys and Compounds

journal homepage: www.elsevier.com/locate/jallcom

Effect of sintering techniques on the microstructure and tensile properties of nano-yttria particulates reinforced magnesium nanocomposites

S.F. Hassan [a,*], Khin Sandar Tun [b], M. Gupta [b]

[a] Department of Mechanical Engineering, King Fahd University of Petroleum & Minerals, P.O. Box 1061, Dhahran 31261, Saudi Arabia
[b] Department of Mechanical Engineering, National University of Singapore, 9 Engineering Drive 1, 117575 Singapore

ARTICLE INFO

Article history:
Received 13 October 2010
Received in revised form 4 January 2011
Accepted 8 January 2011
Available online 14 January 2011

Keywords:
Nano-particulates
Magnesium
Composite
Tensile properties
Ductility

ABSTRACT

In the present study, magnesium nanocomposites were fabricated using magnesium as matrix and nano-yttria as reinforcement. Nanocomposites with 0.2 and 0.7 vol.% of Y_2O_3 particulates with an average size of 29–50 nm were synthesized blend-press-sinter powder metallurgy technique followed by hot extrusion. Conventional slow heating and microwave assisted rapid heating sintering techniques were used. Microstructural characterization of the materials revealed fairly uniform distribution of reinforcement with the presence of minimal porosity in all of the processed materials, while significant grain refinement in the cases of conventionally sintered materials. Tensile properties characterization of the conventional and microwave sintered nanocomposites revealed that significant and resembling increase in the 0.2% yield strength and ultimate tensile strength of magnesium matrix with the increasing presence of reinforcement. The ductility and work of fracture of magnesium matrix increased significantly in the case of conventionally sintered nanocomposites when compared to the microwave assisted sintered nanocomposites.

1. Introduction

Magnesium based composites are getting increasing attention as a result of significant improvement achieved in many properties using discontinuous reinforcement beyond the limits dictated by traditional alloying [1–3]. The end properties of composite materials are critically governed by the selection of type and size of reinforcement and its compatibility with metallic matrix during materials processing. The main drawbacks of magnesium based materials are their low ductility and toughness which in recent time has successfully been improved using various particulates including the nano-size Y_2O_3 [4,5]. Results of the literature search indicated that yttria reinforcement in particulate form in magnesium matrix has been investigated to a limited extent. Graces et al. investigated the microstructure, tensile and compressive properties to correlate the mechanical anisotropy with texture of magnesium matrix reinforced with micron size yttria reinforcements of two different sizes up to 20 vol.% [6]. Han and Dunand reported microstructure, room temperature tensile and compressive properties and creep of dispersion-strengthened-cast magnesium (DSC-Mg) containing 30 vol.% of submicron size Y_2O_3 particulates [7,8]. However, Y_2O_3 particulates reinforcement in nano-size investigated has convincingly increased both the strength and the ductility of magnesium simultaneously. Y_2O_3 particulates are thermodynamically stabile at elevated temperatures and the thermal stability of yttria in magnesium suggests minimal reaction between matrix and reinforcement leading to good interfacial integrity [9]. The limited number of study on nano-size Y_2O_3 particulates reinforced magnesium composites shows powder metallurgy is an important processing route for the materials. In the powder metallurgy processing route sintering is considered to be one of the most essential steps to achieve atomic diffusion induced mechanical integrity and minimal porosity in the structure of the processed materials [10]. Effectiveness of the sintering procedure is critically dependent on the temperature, time, heating rate and environments and hence it is necessary to have a comprehensive study of the different sintering procedures on the end properties of the newly developed magnesium–yttria nanocomposites. Accordingly, the primary aim of the present study was to synthesize the Mg–Y_2O_3 nanocomposites applying powder metallurgy technique using conventional sintering and innovative microwave assisted rapid sintering coupled with hot extrusion. Obtained nanocomposites were characterized for their microstructural characteristics and tensile properties. Particular emphasis was placed to study the effect of sintering processing and the presence of nano-sized Y_2O_3 particulates as reinforcement on the microstructure and tensile response of commercially pure magnesium matrix.

* Corresponding author Tel.: +966 38607787; fax: +966 38602949.
E-mail addresses: sfhassan@kfupm.edu.sa, itsforfida@gmail.com (S.F. Hassan).

0925-8388/$ – see front matter © 2011 Elsevier B.V. All rights reserved.
doi:10.1016/j.jallcom.2011.01.064

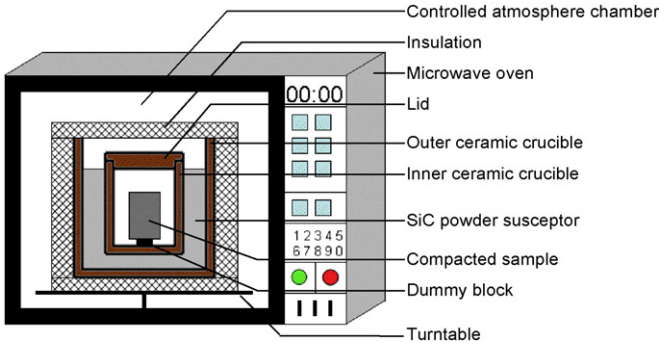

Fig. 1. Schematic diagram of experimental setup for microwave sintering technique.

2. Experimental procedures

2.1. Materials

In this study, magnesium powder of ≥98.5% purity with a size range of 60–300 μm (Merck, Germany) was used as the matrix material and yttria (Y_2O_3) with a particulate size range in nanometer was used as reinforcement. Y_2O_3 with 30–50 nm size range (Inframat Advanced Materials, USA) used in the nanocomposites for microwave assisted sintering process and 29 nm size (Nanostructured & Amorphous Materials Inc., USA) used in the nanocomposites for conventional sintering process. The amount of nanosized Y_2O_3 reinforcement was varied from 0.2 to 0.7 vol.%.

2.2. Processing

Monolithic magnesium and magnesium nanocomposites (Mg/Y_2O_3) containing 0.2 and 0.7 vol.% of yttria particulates were synthesized using powder metallurgy technique. The synthesis process involved blending pure magnesium with nanosized Y_2O_3 particulates in: (a) V-blender at 50-rpm for 6-h (reinforcement size 29 nm) and (b) RETSCH PM-400 mechanical alloying machine at 200 rpm for 1 h (reinforcement size was 30–50 nm). No balls or process control agent was used during the blending step. The blended powder mixtures of Mg and Y_2O_3 were then cold compacted at a pressure of 97 bar (50-tons) to form billets of 35-mm diameter and 40-mm height using a 150-ton press.

The preforms blended in V-blender were sintered in tube furnace at 500 °C for 2-h under argon atmosphere. Heating rate used was 10°/min. The preforms blended in RETSCH PM-400 alloying machine were sintered using an innovative hybrid microwave sintering technique [11] and heated for 13 min to a temperature near the melting point of magnesium in a 900 W, 2.45 GHz SHARP microwave oven. The schematic diagram of microwave sintering setup is shown in Fig. 1.

The synthesis of monolithic magnesium was carried out using similar steps without adding reinforcement particulates for comparison purpose. Sintered billets were subsequently hot extruded at a temperature of 350 °C using an extrusion ratio of 25:1.

2.3. Density measurements

The density of extruded Mg and Mg nanocomposites in polished condition was measured using Archimedes' principle. Three samples were randomly selected from extruded rods and were weighed in air and when immersed in distilled water. An A&D ER-182A electronic balance with an accuracy of 0.0001 g was used for recording the weights. Theoretical densities of the samples were calculated using rule-of-mixture principle.

2.4. Microstructural characterization

Microstructural characterization studies were conducted to determine distribution of reinforcement, grain size, grain morphology, and presence of porosity. HITACHI FE-4500 Field Emission Scanning Electron Microscope (FESEM), OLYMPUS metallographic optical microscope and Scion Image Analyzer were used for this purpose.

2.5. X-ray diffraction studies

X-ray diffraction analysis was carried out on the polished extruded Mg and Mg/Y_2O_3 nanocomposite samples using automated Shimadzu LAB-X XRD-6000 diffractometer. The samples were exposed to CuKa radiation (k = 1.54056) at a scanning speed of 2°/min. The Bragg angle and the values of the interplanar spacing (d) obtained were subsequently matched with the standard values for Mg, Y_2O_3 and related phases.

2.6. Tensile characteristics

The tensile properties of the extruded monolithic magnesium and its nanocomposites were determined in accordance with ASTM standard E8M-01. The tensile tests were conducted on round tension test specimens of 5-mm in diameter and 25-mm gauge length using an automated servohydraulic testing machine with a crosshead speed set at 0.254 mm/min. Total of five tensile specimens was tested for each formulation. Stress–strain curves obtained following testing were used to compute work of fractures (area under stress–strain curve) using excel software. Fracture surface characterization studies were carried out on the tensile fractured Mg and Mg/Y_2O_3 samples to investigate the failure mechanisms using JEOL JSM-5600 LV scanning electron microscope.

3. Results

3.1. Macrostructural characteristics

The results of macrostructural characterization on the compacted and extruded monolithic and nanocomposites samples did not reveal the presence of any macrodefects. The outer surfaces were smooth and free of circumferential cracks.

3.2. Density

The density and porosity measurements conducted on the extruded magnesium and its nanocomposites samples are listed in Table 1. The amount of porosity level in all samples remained below 1% indicating the near net shape forming capability of the processing methodologies adopted in this study. However, marginally lower porosity values for the conventionally sintered materials shows its relatively more effectiveness in producing near dense materials.

3.3. Microstructural characteristics

The results of microstructural characterization revealed fairly uniform distribution of nanosized Y_2O_3 particulates with a few clusters as there is increase in volume percentage in reinforcement (see Fig. 2) in the cases of samples prepared with conventional sintering and microwave assisted sintering. The identity of the Y_2O_3 particulates was confirmed through EDS point analysis (see Fig. 3).

Table 1
Results of density, porosity and grain morphology characterization.

Materials	Sintering process	Density (gm/cm^3)	Porosity (%)	Grain morphology	
				Size (μm)	Aspect ratio
Mg	CS	1.74 ± 0.002	0.08	60 ± 10	1.6 ± 0.3
	MS	1.74 ± 0.01	0.13	20 ± 3	1.4 ± 0.1
$Mg/0.2Y_2O_3$	CS	1.75 ± 0.002	0.10	25 ± 3	1.3 ± 0.6
	MS	1.73 ± 0.01	0.87	19 ± 3	1.4 ± 0.2
$Mg/0.7Y_2O_3$	CS	1.76 ± 0.01	0.35	13 ± 2	1.5 ± 0.3
	MS	1.76 ± 0.01	0.35	18 ± 3	1.4 ± 0.2

MS, microwave sintering; CS, conventional sintering.

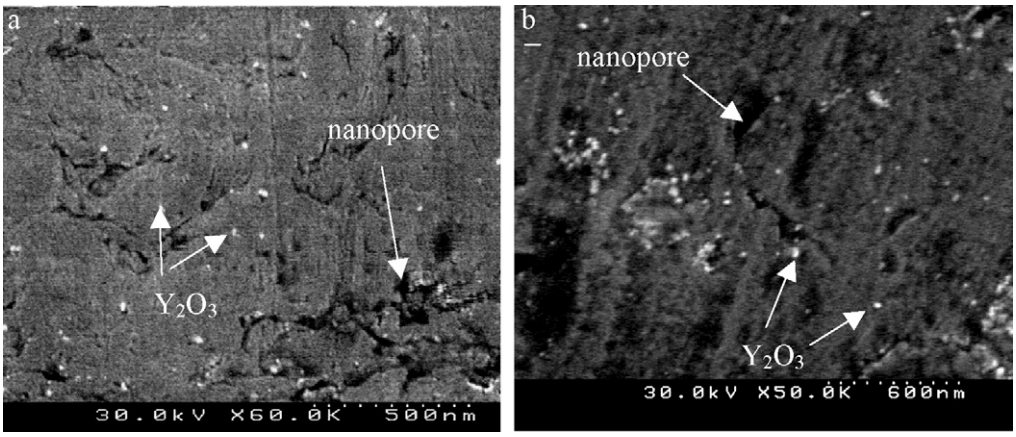

Fig. 2. Representative FESEM micrographs showing reinforcement distribution of Y_2O_3 nano particulates and presence of nanopores in the case of (a) Mg/0.2Y_2O_3 and (b) Mg/0.7Y_2O_3, respectively.

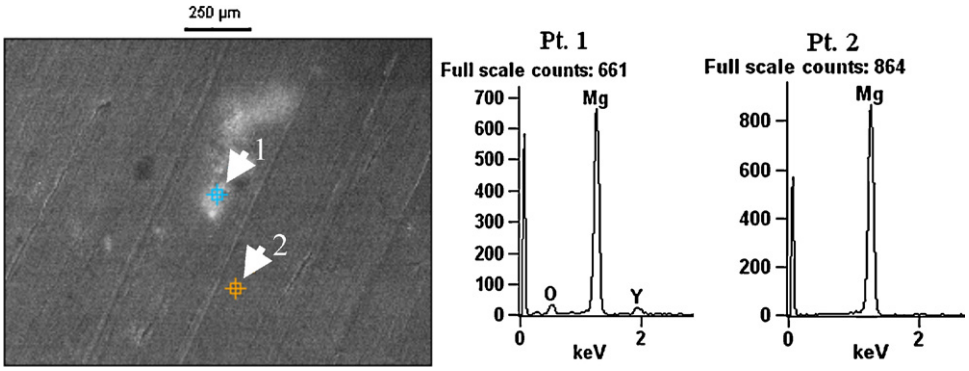

Fig. 3. Typical EDS analysis showing the presence of Y_2O_3 particulates in the case of Mg/0.2Y_2O_3 nanocomposite.

Nanopores were observed in all the nanocomposite samples. The results of grain size and aspect ratio of the extruded samples are shown in Table 1. Near-equiaxed grain morphology was observed for both monolithic and reinforced samples. The results also show that the conventional sintering technique effectively exploited the nanosize Y_2O_3 particulates as grain refiner for the magnesium matrix.

3.4. X-ray diffraction studies

No matching peaks of Y_2O_3, MgO, or other related phases were observed in any samples (see Fig. 4). The absence of the peaks except for that of magnesium may be attributed to the low volume fraction (less than 0.7%) of these phases.

3.5. Tensile characteristics

Tensile characterization studies revealed that 0.2% yield strength, ultimate tensile strength, ductility and work of fracture of the magnesium matrix increased with the incorporation of nanosize Y_2O_3 reinforcement.

The ambient temperature tensile tests conducted on Mg and Mg/Y_2O_3 nanocomposite samples are listed in Table 2 and their representative curves are shown in Fig. 5. The tensile tests results revealed that: (a) Mg/Y_2O_3 nanocomposite samples exhibited superior combination of 0.2% yield strength, UTS and ductility when compared to pure magnesium samples irrespective of their sintering process, (b) the strength values are similar matching for monolithic materials irrespective of their sintering tech-

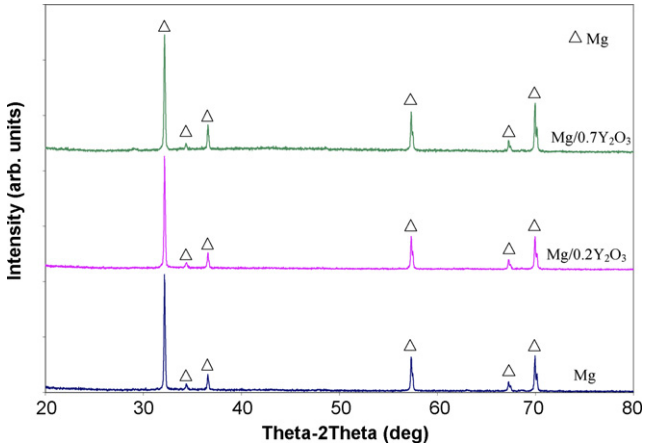

Fig. 4. Representative typical X-ray diffractograms of Mg and Mg/Y_2O_3 nanocomposite samples.

Table 2
Results of room temperature tensile properties of Mg and Mg/Y_2O_3 nanocomposites.

Materials	Sintering process	0.2% YS (MPa)	UTS (MPa)	Ductility (%)
Mg	CS	132 ± 7	193 ± 2	4.2 ± 0.1
	MS	134 ± 7	193 ± 1	7.5 ± 2.5
Mg/0.2Y_2O_3	CS	156 ± 1	211 ± 1	15.8 ± 0.7
	MS	144 ± 2	214 ± 4	8.0 ± 2.8
Mg/0.7Y_2O_3	CS	151 ± 2	202 ± 2	12.0 ± 1.0
	MS	157 ± 10	244 ± 1	8.6 ± 1.2

MS, microwave sintering; CS, conventional sintering.

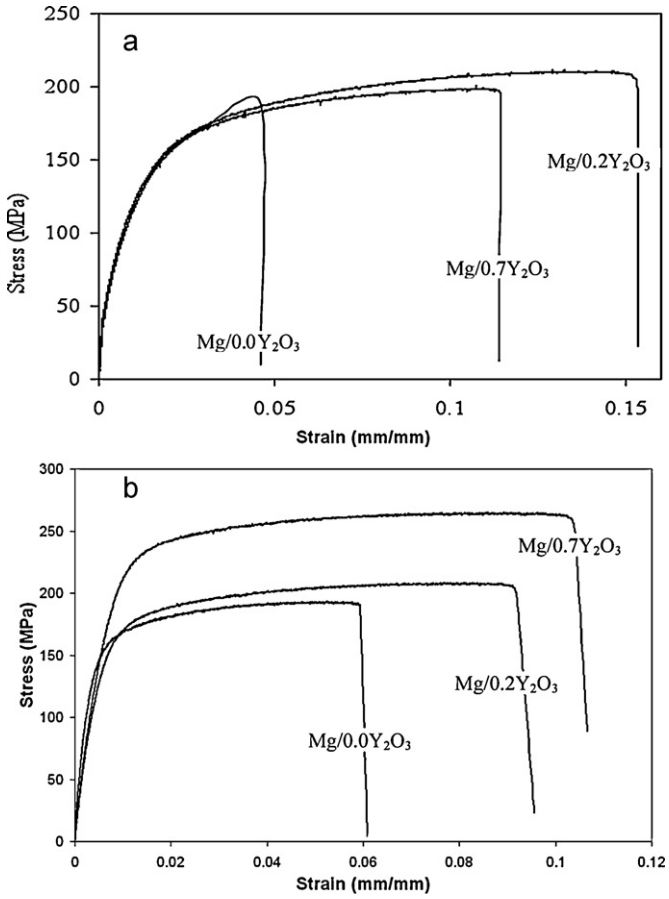

Fig. 5. Representative graphs showing tensile stress–strain behavior of magnesium and nanocomposites sintered using: (a) conventional slow heating and (b) microwave rapid heating, respectively.

niques, (c) strength values of microwave assisted rapid sintered nanocomposite materials are marginally superior to the strength of nanocomposites processed using conventional slow heating sintering, and (d) ductility values are significantly superior for the nanocomposites sintered using conventional slow heating method. The results also revealed that in the case of conventional slow heating sintering the overall tensile properties were reached to the peak with 0.2 vol.% Y_2O_3 reinforcement while in the case of microwave assisted rapid sintering the overall tensile properties increased with increasing volume percentage of nanosized Y_2O_3 reinforcement.

3.6. Fractography

Tensile fracture surfaces of Mg and Mg/Y_2O_3 samples are shown in Fig. 6. Fracture surface of Mg samples indicates the presence of cleavage steps and microscopically rough features. Fracture studies conducted on the nanocomposites samples revealed mixed mode failure showing more evidences of matrix plastic deformation.

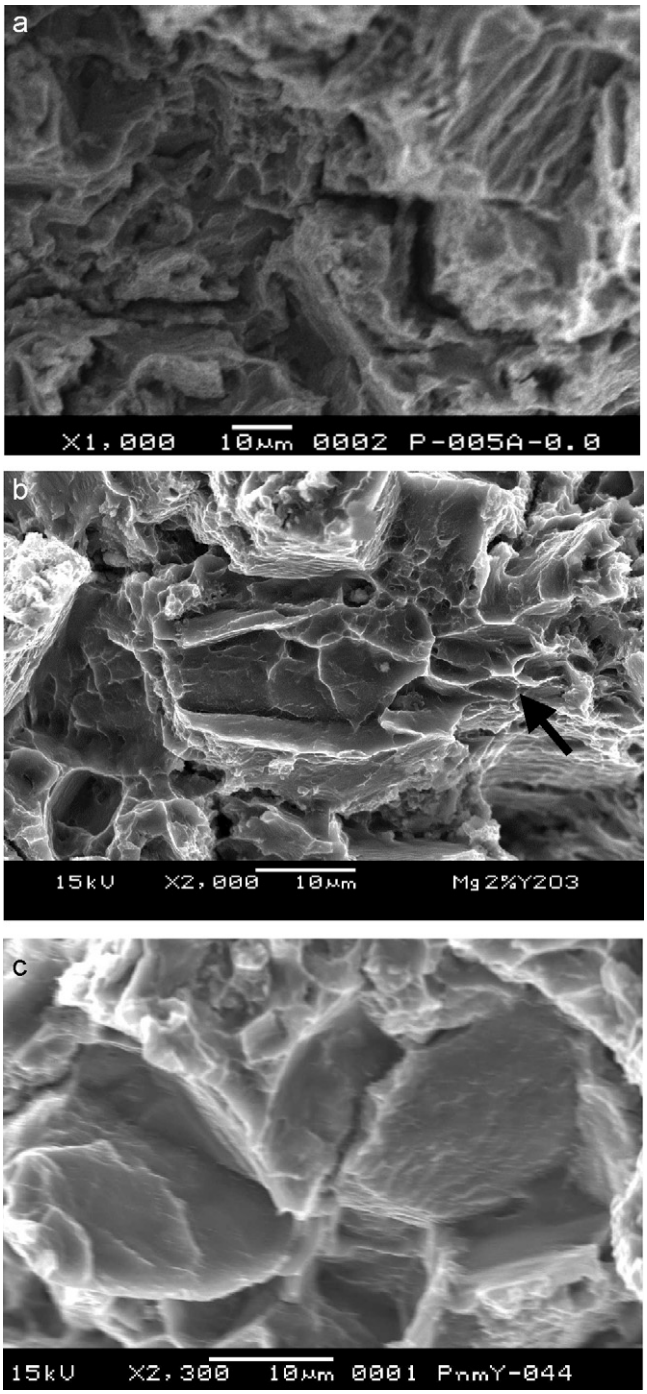

Fig. 6. Representative fractrographs showing: (a) brittle failure in pure Mg, (b) some dimple like features in the case of Mg/2.0Y_2O_3, and (c) intergranular crack propagation in the case of Mg/0.5%Y_2O_3, respectively.

4. Discussion

4.1. Synthesis of Mg and Mg/Y_2O_3 nanocomposites

Synthesis of monolithic Mg and Mg/Y_2O_3 nanocomposites has been successfully accomplished using powder metallurgy route incorporating conventional slow heating and microwave assisted rapid heating sintering techniques following by hot extrusion. The density of both monolithic and nanocomposites samples were greater than 99% indicating the appropriateness of the processing steps and parameters. In particular, the results revealed that energy efficient microwave sintering is equally effective to the conventional sintering in processing these nanocomposite materials. Hence, the microwave assisted rapid sintering is apparently the cost effective choice for synthesize these materials (the conventional sintering, i.e., heating–holding–cooling, required 180 min while it took only 13 min in microwave sintering which translates to cut in ~92.8% of sintering time).

4.2. Microstructural characteristics

Microstructural characterization of extruded nanocomposite samples are discussed in terms of: (a) distribution of reinforcement, (b) reinforcement-matrix interfacial characteristics, (c) grain size and shape, and (d) amount of porosity.

The reasonably uniform distribution of reinforcement particulates (see Fig. 2) can be attributed to: (a) suitable blending parameters and (b) high extrusion ratio used in secondary processing. The two sets of nanocomposites materials were blended using two different systems of blender to homogeneously distribute the nanosize Y_2O_3 particulate reinforcement into the magnesium matrix powder and, interestingly, the results revealed that the high speed rapid blending in mechanical alloying machine and slow speed-long time blending in traditional V-blender are apparently equally effective in dispersion of the reinforcements. The results are encouraging considering the difference in size of Mg powder (60–300 μm) and Y_2O_3 particulates (29–50 nm). Again, theoretically, when secondary processing with a large enough deformation is introduced, homogeneous distribution of reinforcements can be achieved regardless of the size difference between matrix powder and reinforcement particulates [12]. Almost zero standard deviation in density measurement results (see Table 1) also reflect the uniform distribution of the reinforcement in extruded materials. However, there is presence of clusters with the increase in the volume fraction of reinforcement, especially in the traditionally blended nanocomposite. Interfacial integrity between matrix and reinforcement was assessed in terms of interfacial debonding and nanovoids at the particulate-matrix interface and was found to be good as expected from metal/oxide systems [7,13].

Metallography of the extruded samples revealed that the matrix recrystallized completely. The sizes of the near-equiaxed grains of magnesium matrix in the case of nanocomposite samples were smaller when compared to that of unreinforced magnesium (see Table 1). Since Y_2O_3 particulates act as nucleation sites for recrystallized grains during extrusion, the volume fraction of recrystallized grains also rises when the reinforcement volume fraction is increased. However, grain refinement was significant in the case of slow heated conventionally sintered nanocomposites compared to the marginal grain refinement in the case of microwave assisted rapid sintered nanocomposites. This could be attributed to the comparatively finer grain size of the conventionally sintered nanocomposites prior to the extrusion process due to ample time at high temperature for the nanocomposites to completely recrystallized (180 min compare to the 13 min for the microwave sintered nanocomposites).

Microstructural characterization further revealed the presence of almost equiaxed nanopores (see Fig. 2). The pores were not necessarily located with particulate clusters. However, complete recrystallization prior to the extrusion might have reduced further the nanopores in the conventionally sintered nanocomposites while compared with the microwave sintered nanocomposites.

4.3. Tensile characteristics

The results of room temperature tensile testing reveal an increase in 0.2% yield strength, UTS, ductility and work of fracture with the presence of nanosized Y_2O_3 particulates in the magnesium matrix. The best combination of yield and tensile strengths and ductility are observed in the case of: (a) conventionally sintered Mg/0.2Y_2O_3 nanocomposite and (b) microwave sintered Mg/0.7 vol.%Y_2O_3 nanocomposite, respectively.

The contribution of the presence of yttria particles to 0.2% yield stress is due to a number of different mechanisms:

(i) *Strengthening due to the presence of hard second phase:* Increase in yield strength due to the interaction between dislocations and fine particulates, mainly in the cases of oxide dispersion strengthen materials, is where the hard second particulates principally located within grains. In the developed nanocomposites, the oxide particulates are mainly located at the grain boundaries and hence the reinforcement effect due to the Orowan mechanism anticipated being less significant. However, the mechanism might have mentionable effect in the strengthening of Mg/0.2Y_2O_3 nanocomposites due to relatively better distribution of reinforcement and, in particular, for conventionally sintered one due to its finest (29-nm) size of reinforcement.

(ii) *Strengthening due to grain size refinement:* Increase in yield strength with decreasing grain size in accordance with the Hall–Petch relation [10] $\sigma^{HP} = \sigma_o + K/\sqrt{D}$, where σ_o is the friction stress, D is the grain size and K is a constant depends on the stress direction. Strengthening by the Hall–Petch mechanism supposedly high in the cases of conventionally sintered nanocomposite due to significant grain refinement (see Table 1) and negligible the cases of microwave sintered nanocomposites due to marginal grain refinement.

(iii) *Strengthening due to increase in dislocation density:* Dislocation density in the nanocomposite increased due to the mismatch in elastic modulus and coefficient of thermal expansion between matrix and reinforcement and their effect in yield strength increment can be estimated using the following equation [14]:

$$\sigma_{my} = \sigma_{mo} + \Delta\sigma \tag{1}$$

where σ_{my} and σ_{mo} are yield strength of the reinforced and unreinforced matrix, respectively, and $\Delta\sigma$, the total increment in yield stress of the matrix, is given by [15]

$$\Delta\sigma = \sqrt{(\Delta\sigma_{EM})^2 + (\Delta\sigma_{CTE})^2} \tag{2}$$

where $\Delta\sigma_{EM}$ and $\Delta\sigma_{CTE}$ are the incremental stresses due to elastic modulus (EM) mismatch and the coefficient of thermal expansion (CTE) mismatch between the matrix and reinforcement. According to the Taylor dislocation strengthening mechanisms, these stresses can be determined as [14]

$$\Delta\sigma_{EM} = \sqrt{3}\alpha\mu_m b\sqrt{\rho_G^{Em}} \tag{3}$$

$$\Delta\sigma_{CTE} = \sqrt{3}\beta\mu_m b\sqrt{\rho_G^{CTE}} \tag{4}$$

where μ_m is the shear modulus of the matrix, b is Burgers vector and α and β are the two dislocation strengthening coefficients. The presence of reinforcement particulates causes incompatibility in deformation in the matrix through the geometrically necessary dislocations stored near the surfaces of particles. These dislocations are assumed to be generated mainly from the differences in elastic modulus and CTE between Mg matrix and Y_2O_3 particulate reinforcement. The geometrically necessary dislocation density due to elastic modulus mismatch can be estimated by [16]

$$\rho_G^{EM} = \frac{4\gamma}{b\lambda} \tag{5}$$

where γ is the plastic shear strain and λ is the local length scale of the deformation field. For particulate reinforced composites, λ is related to the interparticle distance and considered to be approximately equal to r/f, where r is the particulate radius and f is the volume fraction of the particulates.

When the composites are cooled from the elevated processing temperature, misfit strains or deformations are produced due to the differential thermal contraction at the Mg–Y_2O_3 interface

Table 3
Specific strength and work of fracture of Mg and Mg/Y_2O_3 nanocomposites.

Materials	Sintering process	Work of fracture (MJ/m^3)[a]	$\sigma_{0.2\%YS}/\rho$ (kN-m/kg)	σ_{UTS}/ρ (kN-m/kg)
Mg	CS	7.1 ± 0.3	76	111
	MS	12.9 ± 4.8	77	111
Mg/0.2Y_2O_3	CS	29.3 ± 1.4	89	121
	MS	16.6 ± 4.2	83	124
Mg/0.7Y_2O_3	CS	20.9 ± 2.2	86	115
	MS	21.8 ± 3.1	89	139

MS, microwave sintering; CS, conventional sintering.
[a] Determined from engineering stress–strain diagram using EXCEL software.

[17,18]. Thus, high dislocation density is generated around the particulate reinforcement due to the large difference in CTE between the matrix and reinforcements. These geometrically necessary dislocations needed for the accommodation of thermal misfit strains can be estimated by [19]

$$\rho_G^{CTE} = \frac{A_\varepsilon V_p}{b(1-V_p)d} \quad (6)$$

where A is a geometric constant, b is the Burgers vector, d is the diameter of the particle, V_p is the particle volume fraction and ε is the thermal misfit strain between the matrix and reinforcement. From the above equation, it can also be seen that the smaller the diameter of the particulates and the higher the volume fraction of the reinforcement the higher will be the dislocation density in the matrix. By virtue of significant difference in elastic modulus of Y_2O_3 (177.6 GPa) [20] and Mg (44.7 GPa) [21] (Eq. (5)) and nanosize of Y_2O_3 (Eq. (6)), an increase in dislocation density is expected with increasing amount of Y_2O_3 particles based on fundamental principles. This also indicates a corresponding increase in $\Delta\sigma_{EM}$ and $\Delta\sigma_{CTE}$ thus leading to an increase in yield strength of composite samples (Eqs. (1)–(4) and Table 2).

An improvement of 0.2%YS and UTS over that of pure magnesium was attained for all the materials developed with the addition of Y_2O_3 nano particulates in the current investigation. However, microwave rapid sintering process effectively exploited the strengthening effect of nano-Y_2O_3 and the processed nanocomposites remain marginally superior when compared to the conventionally sintered nanocomposites (see Table 2).

Room temperature tensile tests also revealed the capability of nano-Y_2O_3 particulates reinforcement to increase the ductility of pure magnesium. The increment in ductility of magnesium matrix due to the presence of nano-Y_2O_3 particulates can be attributed primarily to the coupled effect of: (a) grain refinement [22,23], (b) presence of reasonably uniformly distributed reinforcement particulates [24], and (c) slip-on extra non-basal slip system [22,25,26]. Grain refinement particularly benefits hexagonal metals in ductility increment where intergranular fracture arises from intercrystalline stresses [22], and this can be clearly seen in Fig. 6(c). Again, dispersed phases in the brittle matrix, where dislocation mobility is restricted and crack generation is relatively easy, act as ductility enhancers, which is an anomaly to their effect in ductile matrix [24]. Dispersed reinforcement particulates in brittle metal matrix serve to (i) provide sites where cleavage cracks may open ahead of an advancing crack front, (ii) dissipate the stress concentration that would otherwise exist at the crack front, and (iii) alter the local effective state of stress from plane strain to one of the plane stress in the neighborhood of the crack tip. In addition, it has been understood through recent studies that the non-basal slip system activates under axial tensile stress in the fine particle reinforced magnesium matrix and increases ductility [22,25,26]. However, the results indicates that the grain refinement remained as the most effective way to enhance the ductility of magnesium matrix in the developed nanocomposites (see Tables 1 and 2) as the conventionally sintered nanocomposites has significant increment in ductility and the microwave rapid sintered nanocomposites has marginal increment in the ductility. The nominal decrease in ductility in the conventionally sintered nanocomposite with the increasing presence of nano-Y_2O_3 and is due to the increasing presence of porosity [27] (see Table 1) and reinforcement clustering [28]. It may be noted that ductility of all the nanocomposites prepared in this study remained much superior when compared to pure magnesium (see Table 2).

The work of fracture computed using stress–strain diagram reveals that conventionally sintered Mg/Y_2O_3 nanocomposite is distinctly superior when compared to microwave rapid sintered nanocomposites (see Table 3) indicating that the conventional slow heating sintering technique exploited the presence of nano-Y_2O_3 more efficiently and significantly improved the fracture resistance of matrix when compared to microwave rapid heating sintering route.

Considering the properties of base materials, the results revealed the effectiveness of microwave assisted rapid heating sintering technique in improving the strength properties and conventional slow heating sintering technique in improving the ductility and fracture resistance of the developed nanocomposites (see Tables 2 and 3). This also translates microwave rapid sintered nanocomposites are effective for strength based designs (higher yield strength when compared to magnesium) and conventional sintered nanocomposites are effective for damage tolerant designs (higher work of fracture when compared to magnesium).

4.4. Fracture characteristics

The study of uniaxially deformed fracture surfaces of both the microwave and the conventionally sintered materials revealed the microstructural effects on tensile ductility and fracture properties of nano-Y_2O_3 reinforced pure magnesium. Typical brittle fracture surface (Fig. 6a) [29] with the presence of microscopically rough small steps has been seen in the case of magnesium samples. However, fractography of nano-Y_2O_3 reinforced nanocomposite samples revealed salient features such as: (a) ductile fracture of metal with void-sheet mechanism showing dimples [29] (see Fig. 6b) and (b) intergranular crack propagation, typical for hexagonal metal to improve its ductility [22] (see Fig. 6c). It should be noted that the crack propagation features are almost identical in the materials processed by both the microwave rapid heating and the conventional slow heating sintering techniques.

5. Conclusions

(1) Microwave rapid heating sintering and conventional slow heating sintering techniques are equally competent to synthesize nano-Y_2O_3 particulates containing pure magnesium matrix nanocomposites.
(2) Microstructural characterization shows that conventional sintering method is relatively more effective in grain refinement of magnesium matrix when compared to microwave sintered nanocomposites.

(3) Results of tensile behavior characterization revealed that the effect of nano reinforcement is relatively better exploited for strengthening in the cases of microwave sintered nanocomposites and for formability and resistance to fracture in the cases of conventionally sintered nanocomposites.
(4) Fractography revealed that fracture behavior of magnesium matrix changes from brittle to ductile as a result of the presence of nano-Y_2O_3 particulates in both of the materials.

References

[1] H.E. Friedrich, B.L. Mordike, Magnesium Technology: Metallurgy, Design Data, Applications, Springer-Verlag, Berlin Heidelberg, German, 2006.
[2] I.A. Ibrahim, F.A. Mohamed, E.J. Lavernia, Journal of Materials Science 26 (1991) 1137–1156.
[3] D.J. Lloyd, International Materials Reviews 39 (1) (1994) 1–23.
[4] K.S. Tun, M. Gupta, Composites Science and Technology 67 (2007) 2657–2664.
[5] S.F. Hassan, M. Gupta, Journal of Engineering Materials and Technology 123 (3) (2007) 426–467.
[6] G. Garcés, M. Rodríguez, P. Pérez, P. Adeva, Materials Science and Engineering A 419 (2006) 357–364.
[7] B.Q. Han, D.C. Dunand, Materials Science and Engineering A 277 (2000) 297–304.
[8] B.Q. Han, D.C. Dunand, Materials Science and Engineering A 300 (2001) 235–244.
[9] F. Thummler, R. Oberacker, An Introduction to Powder Metallurgy, Institute of Materials, London, 1993.
[10] D. William, Callister, Materials Science and Engineering: An Introduction, John-Wiley & Sons, Inc., New York, USA, 2007.
[11] M. Gupta, W.L.E. Wong, Scripta Materialia 52 (2005) 479–483.
[12] M.J. Tan, X. Zhang, Materials Science and Engineering A 244 (1998) 80–85.
[13] N. Eustathopoulos, M.G. Nicholas, B. Drevet, Wettability at High Temperatures, Pregamon Materials Series, vol. 3, UK, 1999.
[14] L.H. Dai, Z. Ling, Y.L. Bai, Composite Science and Technology 61 (2001) 1057–1063.
[15] T.W. Clyne, P.J. Withers, An Introduction to Metal Matrix Composites, Cambridge University Press, New York, NY, 1993.
[16] N.A. Fleck, G.M. Muller, M.F. Ashby, J.W. Hutchinson, Acta Metallurgica et Materialia 42 (1994) 475–487.
[17] R.J. Arsenault, N. Shi, Materials Science and Engineering A 81 (1986) 175–187.
[18] M. Taya, K.E. Lulay, D.J. Lloyd, Acta Metallurgica et Materialia 39 (1991) 73–87.
[19] N. Chawla, K.K. Chawla, Metal Matrix Composites, Springer Science + Business Media, Inc., New York, 2006.
[20] Website: http://www.ceramics.nist.gov/srd/summary/Y2O3.htm, last assessed October 2010.
[21] A. Buch, Pure Metals Properties: A Scientific-technical Handbook, Materials Park/ASM International/Freund Publishing House, Ohio/London, 1999.
[22] W. Yang, W.B. Lee, Mesoplasticity and its Applications, Springer-Verlag, Berlin, 1993.
[23] G.V. Raynor, The Physical Metallurgy of Magnesium and Its Alloys, Pergamon Press Ltd, Britain, 1959.
[24] R.W. Cahn, Physical Metallurgy, North-Holland Publishing Company, Amsterdam, 1970.
[25] S.F. Hassan, M. Gupta, Materials Science and Technology 20 (2004) 1383–1388.
[26] C.S. Goh, J. Wei, L.C. Lee, M. Gupta, Acta Materialia 55 (2007) 5115–5121.
[27] G.F. Bocchini, International Journal of Powder Metallurgy 22 (3) (1986) 185–202.
[28] G.N. Hassold, E.A. Holm, D.J. Srolovitz, Scripta Metallurgica et Materialia 24 (1990) 101–106.
[29] R.E. Reed-Hill, Physical Metallurgy Principles, 2nd edn., D. Van Nostrand Company, New York, 1964.